

# Annealing Studies on a Fully Cured Epoxy Resin: Effect of Thermal Prehistory, and Time and Temperature of Physical Annealing

K. P. PANG\* and J. K. GILLHAM, *Polymer Materials Program, Department of Chemical Engineering, Princeton University, Princeton, New Jersey 08544-5263*

## Synopsis

The dynamic mechanical behavior at about 1 Hz of a fully cured epoxy resin (maximum glass transition temperature,  $T_{g\infty}$ , ca. 170°C) has been studied during and after isothermal annealing in terms of the influence of thermal prehistory, time of annealing, and temperature of annealing ( $T_a$ ). Annealing temperatures ranged from  $T_g - 15$  to  $T_g - 130^\circ\text{C}$ . The rate of isothermal annealing was observed to decrease by a decade for each decade increase of annealing time when the material was far from equilibrium. Annealing at high temperatures did not measurably affect the material properties during cooling (for  $T \ll T_a$ ); similarly the effect of annealing at low temperatures was not measurable during heating (for  $T \gg T_a$ ).

## INTRODUCTION

Recent studies on the effect of increasing conversion on the density at room temperature ( $\rho_{\text{RT}}$ ) of a diglycidyl ether of bisphenol A (DGEBA) cured with a tetrafunctional aromatic diamine<sup>1,2</sup> have shown that with increased conversion,  $\rho_{\text{RT}}$  increased, reached a maximum in the vicinity of the gel point, and then decreased. The maximum in the  $\rho_{\text{RT}}$  vs. conversion relationship has been discussed<sup>1,2</sup> in terms of: (1) competition between shrinkage due to cure, and loss of contraction on cooling in the rubbery state which is amplified by the nonlinearly increasing glass transition temperature ( $T_g$ ), and (2) physical annealing in the glass transition region being more efficient for materials with lower values of  $T_g$ . This article is concerned mostly with physical annealing of the fully cured epoxy system.

Amorphous materials in the glassy state can be considered to be super-cooled liquids or elastomers whose volume and enthalpy are in excess when compared to the hypothetical equilibrium glass. The slow approaches to equilibrium below  $T_g$  that have been observed, for example, in differential scanning calorimetry (DSC) studies in terms of enthalpy relaxation<sup>1-10</sup> show that the mobility of the molecular chain segments in the glass transition region and in the glassy state is not zero. Sub- $T_g$  annealing studies usually involve prior quenching of materials from an equilibrium state (e.g.,  $T \geq T_g + 20^\circ\text{C}$ ) to a nonequilibrium state (e.g.,  $T < T_g - 20^\circ\text{C}$ )<sup>3-11</sup> which inevitably introduces extra free volume. Since the subsequent densification process involves the gradual decrease of free volume, the thermal prehistory of

\*Present address: Union Carbide Corporation, Somerset, NJ 08875.

an amorphous glass is an important factor in determining the initial submolecular mobility below  $T_g$  and, consequently, the rate of the annealing process.

Given the same rate of cooling, the degree of relaxation on cooling from above  $T_g$  to below  $T_g$  might be expected to be different for materials crosslinked to different extents. Therefore, it is pertinent to study the effect of chemical structure,<sup>10</sup> crosslink density,<sup>11</sup> annealing time and temperature, and thermal prehistory on the annealing process before volume-temperature relationships in the glass state of thermosetting systems can be fully understood.

Investigation of the effects of physical annealing on the density of a fully cured glassy epoxy material has been considered<sup>1,2</sup> using a density gradient column technique, which, however, is only used in the vicinity of RT for measuring density.

Annealing studies of epoxy resins in the glass transition region using torsional creep apparatus<sup>11,12</sup> have shown that the isothermal creep compliance,  $J(t)$ , can be expressed as

$$J(t) = J_0 + (t/t_0)^m \quad (1)$$

where  $J_0$  and  $t_0$  are material parameters which can change with the time of annealing;  $t$  is the time of the creep experiment, and  $m \sim 0.3$ .

Preliminary studies<sup>2</sup> using a torsional braid analyzer (TBA)<sup>13</sup> have indicated that dynamic mechanical analyses are convenient techniques for directly monitoring the physical annealing process over a wide range of annealing temperatures. Effects of different thermal prehistories and annealing times and temperatures on the dynamic mechanical behavior of a fully cured material using the TBA technique are reported here. All experiments for this report were conducted on a single fully cured specimen using the TBA technique which uses a freely oscillating torsion pendulum operating at about 1 Hz.<sup>13</sup> The procedure of using a single specimen depended on being able to reversibly eliminate aging histories by heating the specimen above  $T_g$ . One of the issues that is alluded to in this study is whether the "anomaly," with respect to  $\rho_{RT}$  vs. extent of cure that has been observed in previous studies,<sup>1,2,11,14-23</sup> is due entirely to the nonequilibrium behavior of the material. Future research will deal explicitly with the influence of extent of cure on physical aging and properties.

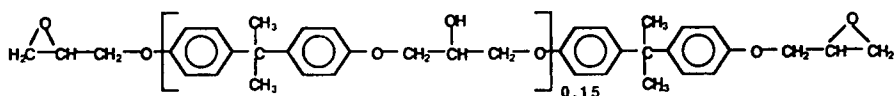
## EXPERIMENTAL

### Materials and Specimen Preparation

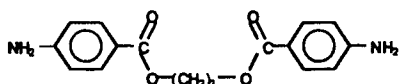
The difunctional epoxy monomer used for this study was a diglycidyl ether of bisphenol A (DER 331, Dow Chemical Co.) which was cured with a tetrafunctional aromatic diamine, trimethylene glycol di-*p*-aminobenzoate ("TMAB," Polar cure 740M, Polaroid Corp.).<sup>1,2,16,24-26</sup> The chemical formulae of the reactants are shown in Figure 1. The materials were reacted stoichiometrically, one epoxy group with one amine hydrogen, according to their respective equivalent weights: DER 331, 190 g/eq; TMAB, 78.5 g/eq.

The reactant mixture was prepared as follows. The difunctional epoxy monomer (a viscous liquid at 25°C) and curing agent (a highly crystalline

## Chemical Formulae



Diglycidyl Ether of Bisphenol A [DER 331]



Trimethylene Glycol Di-p-aminobenzoate [TMAB]

Fig. 1. Chemical formulae of the difunctional epoxy (DER 331)/tetrafunctional aromatic amine (TMAB) system.

solid, mp 125°C) were heated separately in beakers to 140°C. The fluid epoxy monomer was added to the liquid curing agent; the mixture was stirred mechanically for 10 min at 140°C, and then was cooled. A small amount of the mixture (1 g solid/1 mL solvent) was dissolved in methyl ethyl ketone (bp ~ 80°C) for use in torsional braid analysis.<sup>13</sup>

Prior to mounting, the TBA specimen was prepared by dipping a heat-cleaned glass braid into the solution of the reactants. All subsequent treatments were in the TBA apparatus under a slowly flowing atmosphere of helium.

The same epoxy/amine system had been studied using the TBA technique for earlier reports.<sup>25,26</sup> Due to thermal degradation reactions competing with cure at high temperatures,<sup>2,24,26</sup> a methodology was established to obtain the maximum glass transition temperature ( $T_{g\infty} \sim 170^\circ\text{C}$ ) for the present epoxy system,<sup>2,26</sup> which was considered to produce a "fully cured" material. Accordingly, the uncured formulation was reacted isothermally at 80°C for 48 h and then was postcured from 80 to 240°C at 1.1°C/min before being cooled. The subsequent intermittent heating to and cooling from 200°C used for this report did not result in a change in the maximum value of  $T_g$ .

### Annealing Procedure

After "full" cure, the material was taken through the temperature sequence 240 → -170 → 200°C at 1.1°C/min to obtain the dynamic thermomechanical behavior of the "pre-aged" material. It was then cooled from 200°C to the annealing temperature ( $T_a$ ) and the dynamic mechanical properties were monitored isothermally (mostly for 10,000 ± 500 min). Fast-cooled material referred to material that was cooled from 200°C at 11°C/min, whereas

slow-cooled material referred to material that was cooled from 200°C at 1.1°C/min. The temperature of annealing was maintained at  $T_a \pm 0.1^\circ\text{C}$  in dry helium. After annealing, the "aged" material was taken through the temperature sequence  $T_a \rightarrow -170 \rightarrow 200^\circ\text{C}$  at 1.1°C/min to obtain its dynamic thermomechanical spectrum. The thermal history was erased by heating to 200°C. The "rejuvenated" material was then cooled from 200°C at one of the predetermined rates and annealed at another temperature. The procedure was used to generate all of the data for this report.

All the annealing results presented in this study were obtained using a single composite specimen, which was ca. 5 cm long and 1 mm in diameter. The procedure depended on the ability to eliminate induced prehistories by heating above  $T_g$  and, from a subsequent temperature scan at a given cooling rate, to generate an internal standard. One of the advantages of using a single specimen was that the dependence of the relative rigidity on the geometrical parameters (which were unknown) was reproducible and not required. In addition, irreproducibility of data which would inevitably be introduced in reclamping different specimens<sup>27</sup> was eliminated. The use of a glass fiber support also prevented vertical creep under the gravitational load of the pendulum ( $\sim 15$  g). The relative rigidity for different prehistories thus could be compared. However, the specific volume of the material was not measured during the course of isothermal aging (or during temperature scans).

The dynamic thermomechanical spectrum of the "rejuvenated" specimen was found to overlap that of the "pre-aged" specimen for the repeated cycles of the experiment.<sup>2</sup> This is indicative of: (1) the thermoreversibility of the annealing process, (2) no thermal degradation of the material occurred on scanning to and from 200°C, and (3) reproducibility per se.

During a typical TBA experiment, the pendulum is intermittently set into small-angle free oscillations to generate a series of damped waves. Each wave is characterized by a frequency and a decay constant which are related to material behavior through two dynamic mechanical parameters, relative rigidity and logarithmic decrement. The relative rigidity  $1/P^2$  is related to the elastic shear modulus  $G'$ ,

$$G' \approx (8\pi IL/r^4)(1/P^2) \quad (2)$$

where  $r$  and  $L$  are the radius and length of the specimen,  $I$  is the moment of inertia of the oscillating system, and  $P$  is the period of oscillation. The logarithmic decrement is given by  $\Delta \approx \pi G''/G'$ , where  $G''$  is the loss modulus. Due to the composite nature of the TBA specimen, quantitative values of  $G'$  and  $G''$  for the supported material are not obtained.

During the course of isothermal annealing, the relative rigidity can vary as a result of both changing modulus and dimensions of the specimen. The volume of a specimen,  $V$ , can be approximated by that of a regular cylinder, i.e.,  $V = \pi r^2 L$ . As  $L/r \approx 100$ ,

$$V \approx 100\pi r^3 \quad (3)$$

Using eqs. (2) and (3), the relative rigidity at two different states can be

compared:

$$(1/P^2)_2/(1/P^2)_1 = (G'r^4)_2/(G'r^4)_1 \quad (4)$$

$$V_2/V_1 = (r_2/r_1)^3 \quad (5)$$

where subscript 2 stands for more advanced annealing. Combining eqs. (4) and (5) yields

$$(1/P^2)_2/(1/P^2)_1 = (G'_2/G'_1)(V_2/V_1)^{4/3} \quad (6)$$

Since shrinkage occurs during the course of isothermal annealing (i.e.,  $V_2 < V_1$ ), the relative rigidity will actually decrease if not compensated by a corresponding increase in the modulus. In this study, the relative rigidity is observed to increase with time of isothermal annealing. The increase in the modulus term in eq. (6) is therefore more dominant than the decrease in the volume term during isothermal annealing. This can be understood in terms of the more pronounced effect of free volume on the modulus<sup>2,5,11,14,23,28</sup> than on the specific volume. [This argument assumes also that the increase in frequency per se ( $\sim 2\%$ ) during isothermal annealing results in only a minor increase in the modulus.] Dimensional changes also occur on cooling and heating. The relative rigidity in a TBA temperature scan is therefore also a function of the elastic modulus and geometry (as well as frequency).

In principle, the logarithmic decrement ( $\Delta$ ) is independent of the specimen geometry. However, unlike the modulus below  $T_g$ ,  $\Delta$  is not a monotonically varying function of temperature; additional information about either  $G''$  or  $G'$  is required before  $\Delta$  can be analyzed quantitatively.

The automated TBA torsion pendulum system is available from Plastics Analysis Instruments, Inc., P.O. Box 408, Princeton, N.J. 08540.

## RESULTS AND DISCUSSION

### Dynamic Mechanical Properties in the Glassy State: Effect of Cooling Rate

Figure 2 gives two sets of dynamic thermomechanical spectra versus temperature of the fully reacted material, which had been cooled from 200 to  $-170^\circ\text{C}$  at 1.1 (slow-cooled) and  $11^\circ\text{C}/\text{min}$  (fast-cooled), respectively, measured from  $-170$  to  $200^\circ\text{C}$  using a heating rate of  $1.1^\circ\text{C}/\text{min}$ . As plotted, the relative rigidity of the slow- and fast-cooled materials are almost indistinguishable. (The inset of Fig. 2 shows expanded relative rigidity data.) The difference is more discernable in the logarithmic decrement data. The lower relative rigidity and concomitant higher mechanical damping reflect a larger free volume being associated with the fast-cooled material below  $T_g$ . This is a consequence of the decreasing mobility of chain segments on cooling through the glass transition region; thus a higher free volume content upon cooling below the glass transition temperature results for the fast-cooled material. Here, the measurable difference in the relative rigidity at  $25^\circ\text{C}$  is about 0.25%, whereas that at  $130^\circ\text{C}$  is about 1.62%. The corresponding changes in the logarithmic decrement are 12.3 and 40.5%, respectively. [Previous studies<sup>1,2</sup> on

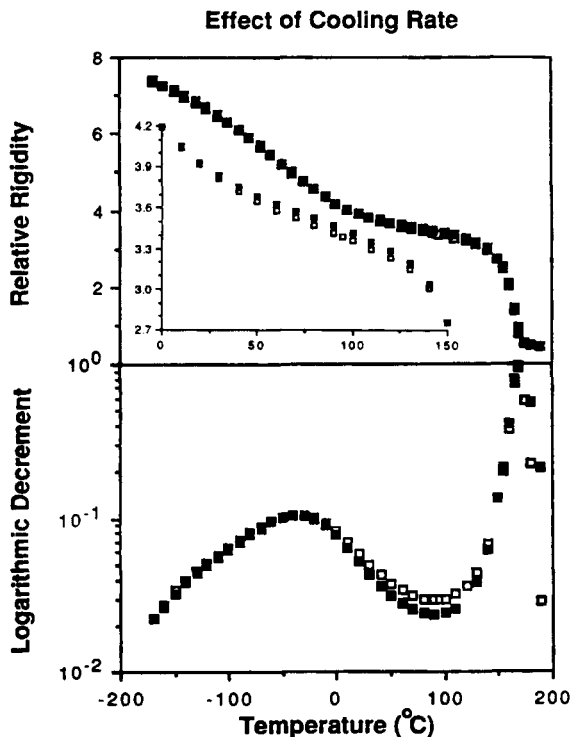


Fig. 2. Dynamic mechanical spectra of fully cured epoxy specimens vs. temperature at a heating rate of  $1.1^{\circ}\text{C}/\text{min}$  from  $-170^{\circ}\text{C}$ . Prehistory: ( $\square$ ) fast-cooled material; ( $\blacksquare$ ) slow-cooled material. Effect of cooling rate from  $200^{\circ}\text{C}$  is discernible in the logarithmic data between  $-30$  and  $130^{\circ}\text{C}$  and in the expanded (inset) relative rigidity data between  $0$  and  $150^{\circ}\text{C}$ .

the same epoxy system have shown that a  $0.04\%$  change in  $RT$  ( $\equiv 24.95^{\circ}\text{C}$ ) density was measurable between a material that was cooled from above  $T_g$  at about  $0.1^{\circ}\text{C}/\text{min}$  and the same material that was quenched from above  $T_g$  (reproducibility ca.  $\pm 0.01\%$ ).

The glass transition temperature is expected to depend on the rate of cooling (and heating) through the transition region. However, from the maxima in the logarithmic decrement,  $T_g$  measured during heating at a constant rate ( $1.1^{\circ}\text{C}/\text{min}$ ) appears to be independent of the prior cooling rate. This is presumably due to the operational procedure of measuring  $T_g$  using the maximum in the logarithmic decrement, which is close to the rubbery end of the glass transition region. Hence, any free volume effect may have been erased on scanning to the assigned value of  $T_g$ . No significant effect of cooling rate on the secondary transition temperature ( $T_{\text{sec}} < T_g$ ) was measurable at the resolution used for presentation of the data.

The fact that cooling rate did not measurably affect the dynamic thermo-mechanical properties below  $T_{\text{sec}}$  is consistent with the notion that the secondary relaxation processes of amorphous polymers involve free volume changes of significantly smaller scale than that required for the rubber to glass transition.<sup>5</sup>

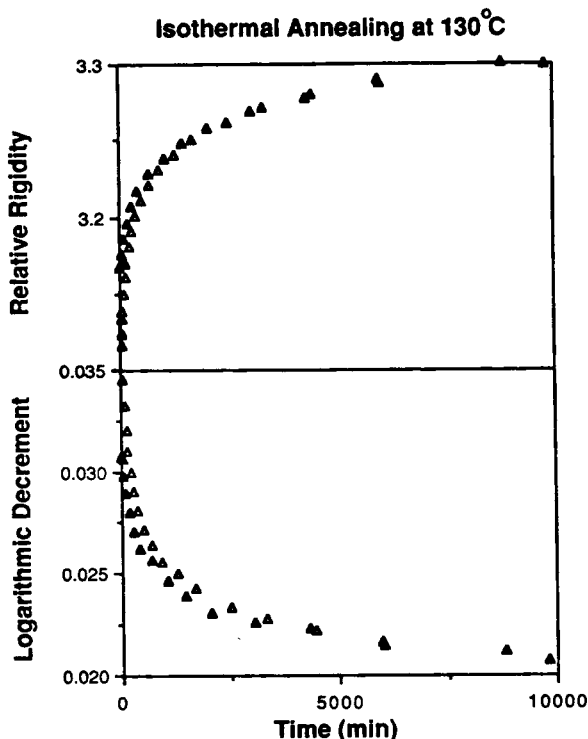


Fig. 3. Dynamic mechanical properties vs. time of isothermal annealing at  $T_a = 130^\circ\text{C}$ : (▲) slow-cooled material; (△) fast-cooled material.

### Isothermal Annealing

During the course of isothermal annealing, the relative rigidity and logarithmic decrement at  $T_a$  were monitored vs. time. After cooling from  $200^\circ\text{C}$ , on average, 20–30 min elapsed before  $T_a$  was controlled to  $\pm 0.1^\circ\text{C}$  (after an initial transient period). The isothermal annealing data given in this report represent those for which the temperature =  $T_a \pm 0.1^\circ\text{C}$ .

Figure 3 displays the relative rigidity and logarithmic decrement of one composite specimen (with the two different thermal prehistories) vs. time at an annealing temperature of  $130^\circ\text{C}$ . The relative rigidity is observed to increase with time as a result of the spontaneous densification of the material, whereas the logarithmic decrement is observed to decrease with time.<sup>27</sup> The fast-cooled material, with an initially lower relative rigidity corresponding to an initially higher free volume, is being annealed initially at a faster rate than the slow-cooled material. A complementary pattern is observed for the logarithmic decrement. At long times of annealing ( $\sim 10000$  min), the relative rigidity and logarithmic decrement trajectories of the fast- and slow-cooled materials appear to merge.

Figure 4 shows isothermal annealing data vs. linear time at annealing temperatures ranging from  $39$  to  $155^\circ\text{C}$ . In general, most of the annealing occurs during the early stages when the free volume content is highest. The relative rigidity can reach an equilibrium value when the annealing tempera-

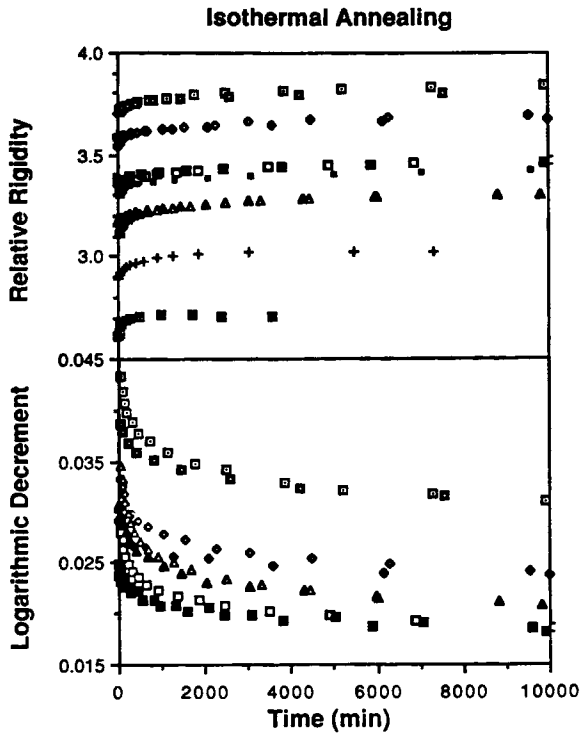


Fig. 4. Dynamic mechanical properties vs. linear time of isothermal annealing at various  $T_a$ 's and thermal prehistories: (⊞) 39°C, fast-cooled; (□) 39°C, slow-cooled; (◇) 59°C, fast-cooled; (◆) 59°C, slow-cooled; (□) 100°C, fast-cooled; (■) 100°C, slow-cooled; (■) 110°C, slow-cooled; (△) 130°C, fast-cooled; (▲) 130°C, slow-cooled; (+) 150°C, slow-cooled; (⊞) 155°C, fast-cooled. (For clarity, the logarithmic decrement vs. time data at  $T_a = 110, 150,$  and  $155^\circ\text{C}$  is not shown.)

ture is close to  $T_g$ . For example, for  $T_a = 155^\circ\text{C}$ , an equilibrium value of the relative rigidity can be reached in about 1000 min.

When the annealing data in Figure 4 are replotted vs. log time, as shown in Figure 5, approximately straight lines are obtained for the relative rigidity data (particularly at long times). That is, for each  $T_a$ ,

$$1/P^2 = a + b \log_{10} t \quad (7)$$

where  $a$  and  $b$  are constants and  $t$  is the time of annealing. The enthalpy relaxation,<sup>6,8-10</sup> stress-relaxation,<sup>6,8</sup> creep compliance,<sup>12</sup> and specific volume<sup>8,12</sup> of epoxy resins have also been found to change lineary with log time of physical aging. From eq. (7), the rate of annealing at each  $T_a$  (and for the different thermal prehistories) can be estimated as a function of time

$$d(1/P^2)/dt = 2.303b/t \quad (8)$$

Figure 6 shows the dependence of annealing rate on the time of annealing at  $T_a = 130^\circ\text{C}$  for fast- and slow-cooled materials on a log-log plot. The fast-cooled material has a higher rate of annealing in the early stages due to a higher initial free volume content. With increasing time of annealing, the rates of annealing for the fast- and slow-cooled materials appear to merge.



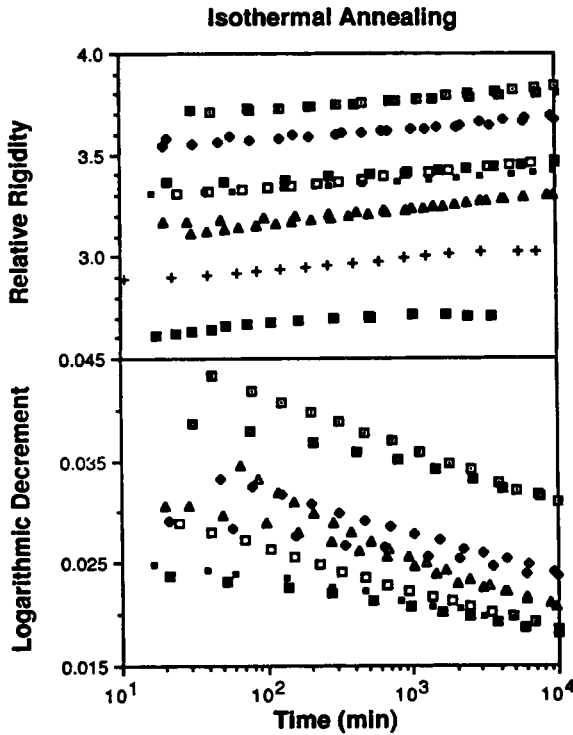


Fig. 5. Dynamic mechanical properties vs. log time of isothermal annealing at various  $T_a$ 's and thermal prehistories: (■) 39°C, fast-cooled; (□) 39°C, slow-cooled; (◇) 59°C, fast-cooled; (◆) 59°C, slow-cooled; (◻) 100°C, fast-cooled; (■) 100°C, slow-cooled; (■) 110°C, slow-cooled; (△) 130°C, fast-cooled; (▲) 130°C, slow-cooled; (+) 150°C, slow-cooled; (⊞) 155°C, fast-cooled. (For clarity, the logarithmic decrement vs. time data at  $T_a = 150$  and  $155^\circ\text{C}$  is not shown.)

Figure 7 summarizes the dependence of rate of annealing on the time of annealing at different isothermal temperatures on a log-log plot for fast-cooled ( $T_a = 39, 130,$  and  $155^\circ\text{C}$ ) and slow-cooled materials ( $T_a = 39, 130,$  and  $150^\circ\text{C}$ ). At the beginning of annealing, the rate of annealing is higher at higher annealing temperatures. Nevertheless, the physical aging process is a complex function of free volume and temperature. For example, crossover behavior can be observed at high annealing temperatures for  $T_a = 150$  (slow-cooled) and  $155^\circ\text{C}$  (fast-cooled) at long times. The rate of annealing decreases substantially as the free volume approaches an equilibrium value at  $T_a$ . In general, the rate of annealing decreases with time of aging as a consequence of decreasing free volume. When the material is far from equilibrium, the slopes of the approximate straight lines are ca.  $-1$ , i.e.,

$$d(\log R_a)/d(\log t) \sim -1 \quad (9)$$

where  $R_a = d(1/P^2)/dt$ . That is, the log rate of annealing decreases by a decade for each decade increase of annealing time.<sup>5,11,29</sup>

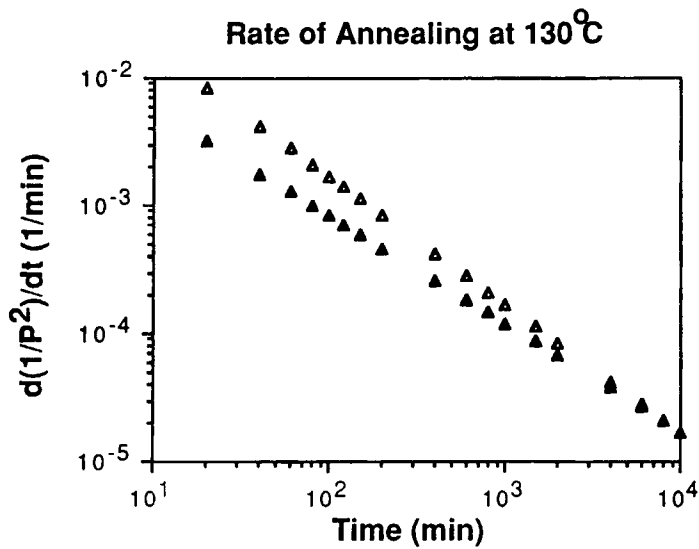


Fig. 6. Calculated rate of annealing vs. time of isothermal annealing at  $T_a = 130^\circ\text{C}$ : ( $\Delta$ ) fast-cooled; ( $\blacktriangle$ ) slow-cooled.

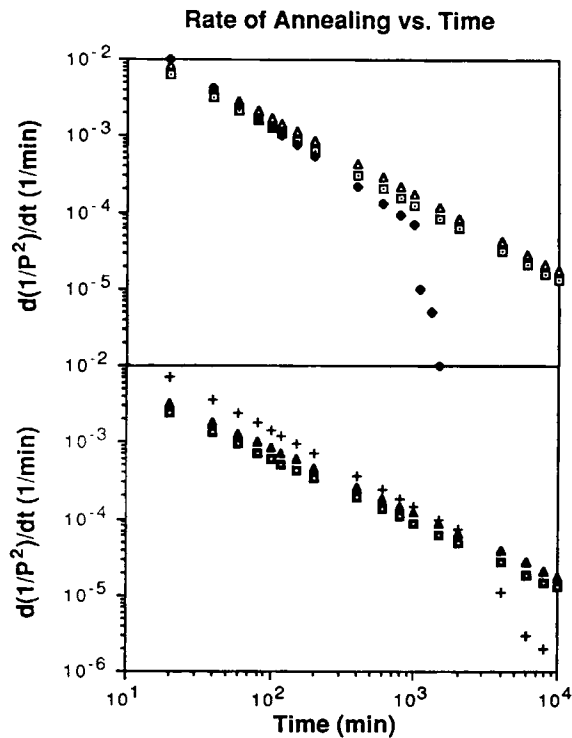


Fig. 7. Rates of annealing vs. time of isothermal annealing at various  $T_a$ 's for fast-cooled (top) and slow-cooled (bottom) materials: ( $\square$ )  $39^\circ\text{C}$ , fast-cooled; ( $\blacktriangle$ )  $130^\circ\text{C}$ , fast-cooled; ( $\blacklozenge$ )  $155^\circ\text{C}$ , fast-cooled; ( $\square$ )  $39^\circ\text{C}$ , slow-cooled; ( $\blacktriangle$ )  $130^\circ\text{C}$ , slow-cooled, (+)  $150^\circ\text{C}$ , slow-cooled.

### Effect of Annealing on the Dynamic Thermomechanical Properties

After isothermal annealing, the material was taken through the temperature sequence  $T_a \rightarrow -170 \rightarrow 200^\circ\text{C}$  at  $1.1^\circ\text{C}/\text{min}$  to obtain the dynamic thermomechanical properties of the aged material. Figure 8(a) summarizes the relative rigidity vs. temperature data from 0 to  $160^\circ\text{C}$  for  $T_a$  ranging from 39 to  $155^\circ\text{C}$ . Figure 8(b) summarizes the corresponding logarithmic decrement vs. temperature data. Corresponding dynamic thermomechanical data have been averaged for the cooling scan from  $T_a$  to  $-170^\circ\text{C}$  and the heating scan from  $-170 \rightarrow 200^\circ\text{C}$ . Also shown in Figs. 8(a) and 8(b) are the dynamic thermomechanical properties of the pre-aged material measured at  $1.1^\circ\text{C}/\text{min}$ , for which corresponding increasing and decreasing temperature data have been averaged during a scan from  $200 \rightarrow -170 \rightarrow 200^\circ\text{C}$ . The time of annealing was ca.  $10000 \pm 500$  min for  $T_a = 39$  to  $130^\circ\text{C}$ ; times of annealing were less for  $T_a = 150$  and  $155^\circ\text{C}$ .

The changes in the relative rigidity after annealing, as compared to the pre-aged material, measured at  $T_a$  range from 2.5% at  $39^\circ\text{C}$  to 4.8% at  $150^\circ\text{C}$ . The corresponding changes in the logarithmic decrement range from  $-19.7\%$  at  $39^\circ\text{C}$  to  $-50\%$  at  $150^\circ\text{C}$ . Apparently, the logarithmic decrement is a more sensitive parameter than the relative rigidity for monitoring the annealing process. From the logarithmic decrement data, there appears to be a range from below to above  $T_a$ , beyond which aging has negligible apparent effect on the dynamic mechanical properties. This affected range ( $\Delta T$ ) is given in Table I. This is in contrast with the reported annealing studies on epoxy resins<sup>7</sup> and composites<sup>8</sup> for which aged materials displayed significantly higher modulus over the entire temperature range in the glassy state. [On further expansion of scales (above that used for the inset of Fig. 2), the relative rigidity data do reveal small but definite differences throughout the temperature range of the glassy state.<sup>30</sup>] The dependence of the operational range on the time of isothermal annealing has not been investigated for this report. Nevertheless, from the dynamic thermomechanical spectra shown in Figure 2, it is unlikely that physical aging ( $T_a \geq 39^\circ\text{C}$ ) will measurably affect the secondary relaxation processes (i.e.,  $T \ll T_g$ ) of amorphous polymers.<sup>5</sup>

As shown in Figures 4, 5, and 7, the leveling off of the relative rigidity at  $T_a = 155^\circ\text{C}$  at long time indicates that the free volume of the material is approaching a minimum (equilibrium) value. Upon subsequent cooling from  $155^\circ\text{C}$ , the slower relaxation rate compared with the rate of cooling does not allow annealing to occur at  $T \ll 155^\circ\text{C}$ . As observed in Figures 8(a) and 8(b), the dynamic thermomechanical spectra of the aged and pre-aged materials overlap at lower temperatures ( $T \ll T_a$ ). Therefore, the effect of aging at higher temperatures is not measurable (at the sensitivity level used) on cooling to  $T \ll T_a$ .

Furthermore, the effect of annealing at, e.g.,  $T_a = 39^\circ\text{C}$ , was not observed upon heating to  $T > 39 + 40^\circ\text{C}$ . This can be understood in terms of the free volume increases and the relaxation time decreases with increasing temperature during measurement.<sup>10</sup>

The glass transition and secondary transition temperatures, which are measured by the maxima in the logarithmic decrement, do not appear to be

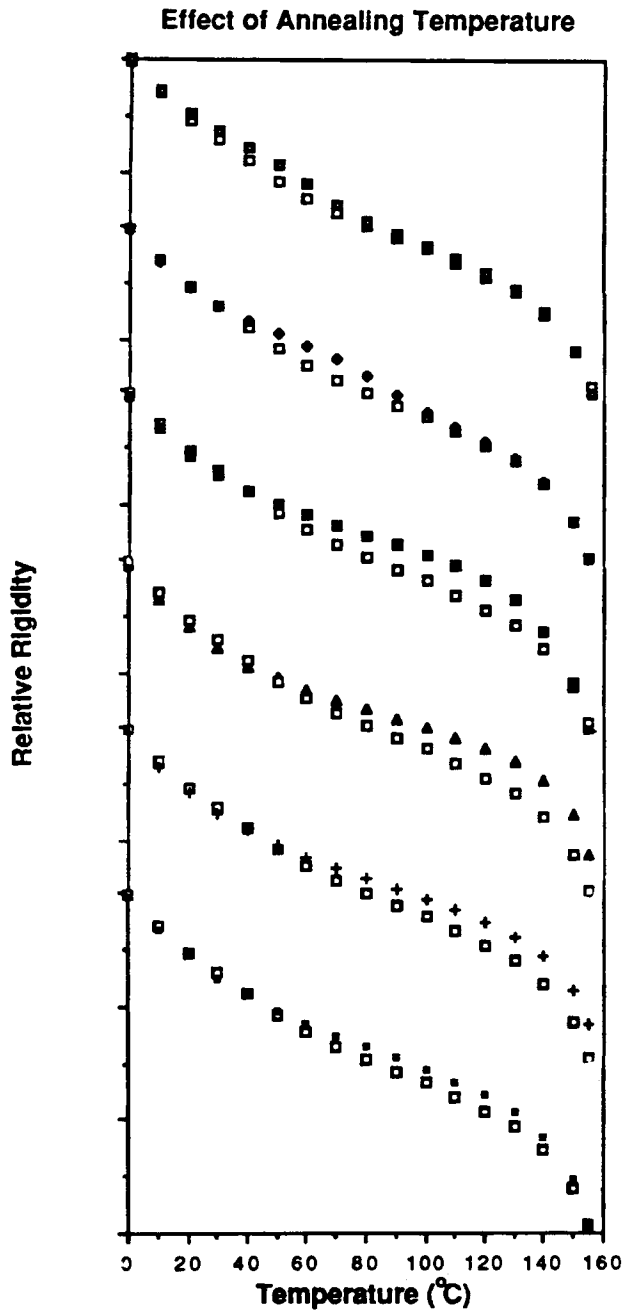


Fig. 8(a). Relative rigidity vs. temperature of pre-aged ( $\square$ ) and aged materials after isothermal annealing at various  $T_a$ 's: ( $\square$ ) 39°C, slow-cooled; ( $\blacklozenge$ ) 59°C, slow-cooled; ( $\blacksquare$ ) 110°C, slow-cooled; ( $\blacktriangle$ ) 130°C, slow-cooled; (+) 150°C, slow-cooled; ( $\blacksquare$ ) 155°C, fast-cooled. Scanning rate: 1.1°C/min in dry helium.

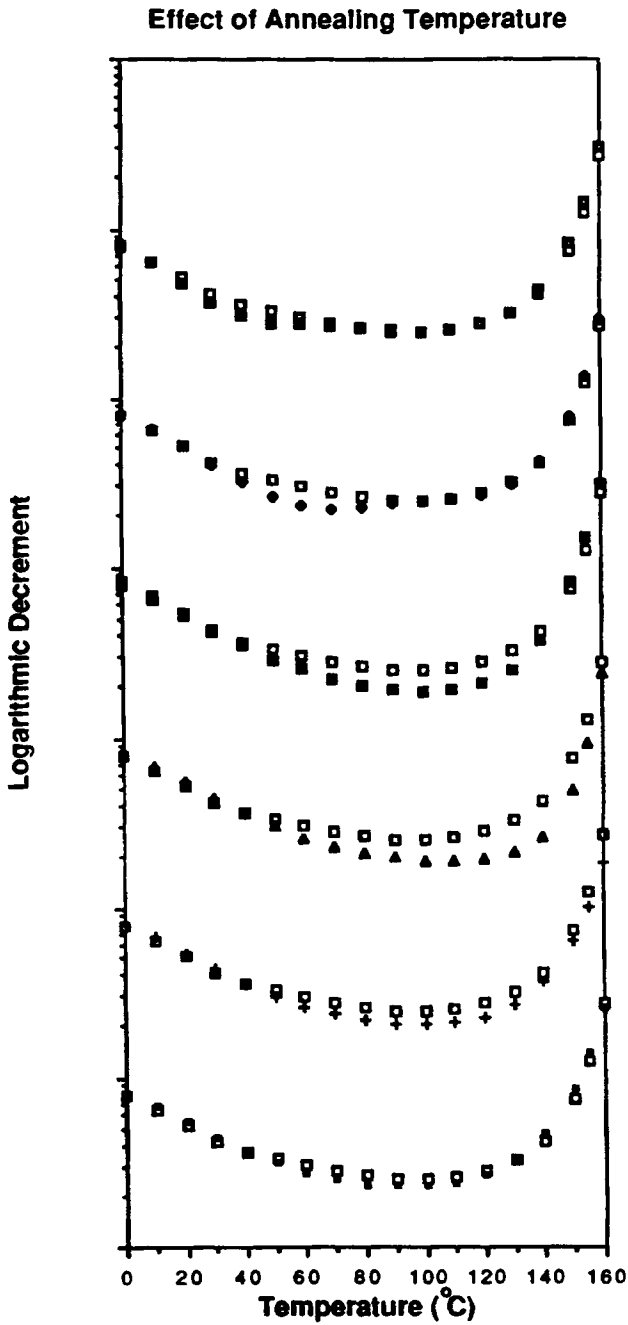


Fig. 8(b). Logarithmic decrement vs. temperature of pre-aged ( $\square$ ) and aged materials after isothermal annealing at various  $T_a$ 's: ( $\square$ ) 39°C, slow-cooled; ( $\blacklozenge$ ) 59°C, slow-cooled; ( $\blacksquare$ ) 110°C, slow-cooled; ( $\blacktriangle$ ) 130°C, slow-cooled; (+) 150°C, slow-cooled; ( $\bullet$ ) 155°C, fast-cooled. Scanning rate: 1.1°C/min in dry helium.

TABLE I  
Temperature Range ( $\Delta T$ ) of Affected Behavior vs.  
Annealing Temperature ( $T_a$ )

$T_a$ (°C)	$\Delta T$ (°C)
39	$T_a - 30$ to $T_a + 40$
59	$T_a - 30$ to $T_a + 40$
110	$T_a - 70$ to $T_a + 40$
130	$T_a - 80$ to $T_a + 30$
150	$T_a - 100$ to $T_a + 10$
155	$T_a - 105$ to $T_a + 5$

significantly affected by physical annealing. As discussed earlier, due to the operational procedure of measuring  $T_g$  which is located close to the rubbery end of the glass transition, any effect due to physical aging may have been erased during scanning to  $T_g$ .<sup>2</sup> Other physical aging studies on epoxy resins have indicated that the glass transition<sup>6,8,9</sup> and secondary transition<sup>9</sup> temperatures increased with aging time. If the assigned  $T_g$  is located close to the glassy end of the glass transition region, it is expected then to be affected by physical aging.

#### Effect of Physical Annealing on the Anomalous Room Temperature Rigidity

Figure 9 displays the dynamic thermomechanical spectra of partially and postcured states of the same composite specimen. (The partially cured material was cured isothermally at 80°C; in the process physical aging also occurred for ca. 23 h after vitrification.) [The dynamic thermomechanical data were obtained during a heating scan from -170°C at 1.1°C/min after cooling from 80 and 200°C, respectively, to -170°C at 1.1°C/min.] The anomalous behavior below  $T_g$  can be observed: The relative rigidity in the glassy state decreases with increasing  $T_g$ . (The anomaly does not depend on vitrification occurring during cure.)

Using eq. (7), the time of annealing required to increase the relative rigidity of the postcured material to the level of the partially cured material can be estimated. For example, at  $T_a = 39^\circ\text{C}$ , eq. (7) becomes

$$1/P^2 = 3.617 + 0.054427 \log t \quad (10)$$

Hence,  $t \sim 2 \times 10^{19}$  min for  $1/P^2$  to increase from 3.617 to 4.667. Similarly, at  $T_a = 59^\circ\text{C}$ ,  $t \sim 3 \times 10^{17}$  min for  $1/P^2$  to increase from 3.449 to 4.529. These calculated figures reflect the relaxation times of the material deep in the glassy state which can be predicted by molecular kinetic theories in the literature.<sup>31-33</sup>

The above calculations, as well as the results of Figures 8(a) and 8(b) which show that isothermal annealing in the glass transition region only marginally affects the modulus well below  $T_g$ , indicate that the anomalous behavior of room temperature density cannot be accounted for by physical aging either at  $T_a (= RT) \ll T_g$  or at  $T_a (> RT) \sim T_g$ .

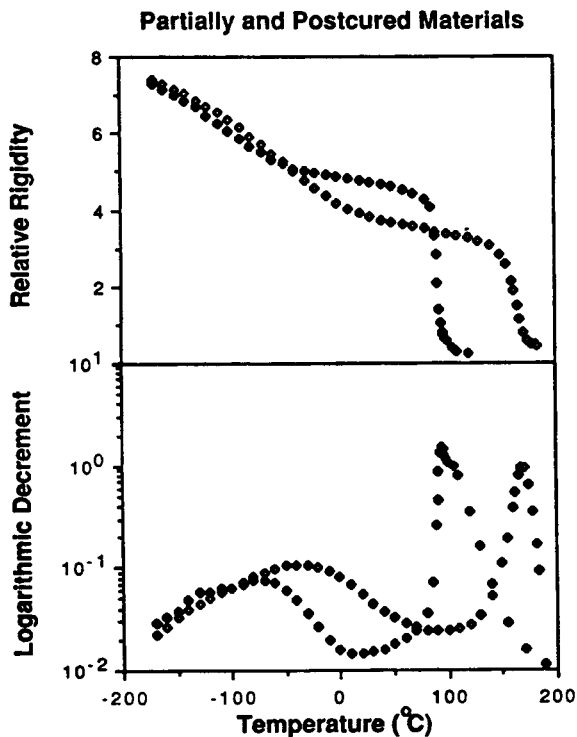


Fig. 9. Dynamic thermomechanical spectra of partially ( $\blacklozenge$ ) and postcured ( $\diamond$ ) materials between  $-170$  and  $200^\circ\text{C}$ . Scanning rate:  $1.1^\circ\text{C}/\text{min}$  in dry helium.

## CONCLUSIONS

The dynamic mechanical behavior of a fully cured diglycidyl ether of bisphenol A reacted with a tetrafunctional aromatic amine has been studied during and after isothermal annealing in terms of thermal prehistories, and time and temperature of annealing, using a torsional braid analyzer (TBA).

The relative rigidity is observed to increase linearly with log time of annealing, whereas the logarithmic decrement is observed to decrease with time of annealing, as the consequence of the spontaneous densification of the material in the glassy state. The rate of isothermal annealing of a material fast-cooled from an equilibrium state is higher in the early stages of annealing in comparison with a slow-cooled material. This is due to a higher initial free volume content for the former. With increasing time of isothermal annealing (decreasing free volume), the rates of annealing of both fast- and slow-cooled materials become indistinguishable. In general, the rate of annealing decreases by a decade for every decade increase in time of annealing.

Annealing at high temperatures does not measurably affect the thermomechanical behavior during cooling (for  $T \ll T_a$ ). Similarly, the effect of annealing at low temperatures was not observed during heating in a temperature scan (for  $T \gg T_a$ ). The former suggests that physical aging is not responsible for the anomalous behavior of thermosetting systems in which the  $RT$  modulus and density decrease with the extent of cure.

Financial support has been provided by the Office of Naval Research.

### References

1. K. P. Pang and J. K. Gillham, *Proc. Am. Chem. Soc., Div. Polym. Mater. Sci. Eng.*, **56**, 435, 1987; *J. Appl. Polym. Sci.*, **37**, 1969 (1989).
2. K. P. Pang, Ph.D. dissertation, Department of Chemical Engineering, Princeton University, 1989.
3. A. J. Kovacs, *J. Polym. Sci.*, **30**, 131 (1958).
4. S. E. B. Petrie, *Bull. Am. Phys. Soc.*, **17**, 373 (1972).
5. L. C. E. Struik, *Physical Aging in Amorphous Polymers and Other Materials*, Elsevier, Amsterdam, 1978.
6. Z. H. Ophir, J. A. Emerson, and G. L. Wilkes, *J. Appl. Phys.*, **49**, 5032 (1978).
7. J. Kaiser, *Makromol. Chem.*, **108**, 573 (1979).
8. E. S. W. Kong, *Epoxy Resins and Composites IV*, K. Dusek, Ed., Advances in Polymer Science, Vol. 80, Springer-Verlag, New York, 1986, pp. 125-172.
9. J. Mijovic and K. F. Lin, *J. Appl. Polym. Sci.*, **32**, 3211 (1986).
10. Y. G. Lin, H. Sautereau, and J. P. Pascault, *J. Appl. Polym. Sci.*, **32**, 4595 (1986).
11. I. C. Choy, Ph.D. dissertation, Materials Science and Engineering Department, University of Pittsburgh, 1987.
12. J. M. Augl, *J. Rheol.*, **31**(1), 1 (1987).
13. J. B. Enns and J. K. Gillham, *Am. Chem. Soc., Adv. Chem. Ser.*, **203**, 27 (1983).
14. J. P. Aherne, J. B. Enns, M. J. Doyle, and J. K. Gillham, *Am. Chem. Soc., Div. Org. Coat. Plast. Chem. Prepr.*, **46**, 574 (1982).
15. J. B. Enns and J. K. Gillham, *J. Appl. Polym. Sci.*, **28**, 2831 (1983).
16. M. T. Aronhime, X. Peng, and J. K. Gillham, *J. Appl. Polym. Sci.*, **32**, 3589 (1986).
17. A. Shimazaki, *J. Polym. Sci., Part C*, **23**, 555 (1968).
18. W. Fisch, W. Hofman, and R. Schmid, *J. Appl. Polym. Sci.*, **13**, 295 (1969).
19. G. A. Pogany, *Polymer*, **11**, 66 (1970).
20. K. Suzuki, Y. Miyano, and T. Kunio, *J. Appl. Polym. Sci.*, **21**, 3367 (1977).
21. V. B. Gupta, L. T. Drzal, and M. J. Rich, *J. Appl. Polym. Sci.*, **30**, 4467 (1985).
22. D. A. Shimp, *Proc. Am. Chem. Soc., Div. Polym. Mater. Sci. Eng.*, **54**, 107 (1986).
23. A. Noordam, J. J. M. H. Wintraecken, and G. Walton, *Crosslinked Epoxies*, B. Sedlacek and J. Kahovec, Eds., Walter de Gruyter, New York, 1987, pp. 373-389.
24. L. C. Chan, H. N. Naé, and J. K. Gillham, *J. Appl. Polym. Sci.*, **29**, 3307 (1984).
25. X. Peng and J. K. Gillham, *J. Appl. Polym. Sci.*, **30**, 4685 (1985).
26. K. P. Pang and J. K. Gillham, *Proc. Am. Chem. Soc., Div. Polym. Mater. Sci. Eng.*, **55**, 65, 1986; *J. Appl. Polym. Sci.*, to appear.
27. S. E. B. Petrie, *Physical Structure of the Amorphous State*, G. Allen and S. E. B. Petrie, Eds., Marcel Dekker, New York, 1977, pp. 225-247.
28. R. N. Haward and J. R. McCallum, *Polymer*, **12**, 189 (1971).
29. S. Matsuoka, H. E. Blair, S. S. Bearder, H. E. Kern, and J. T. Ryan, *Polym. Eng. Sci.*, **18**, 1073 (1978).
30. G. Wisanrakkit and J. K. Gillham, *Proceedings, Society of Plastics Engineers Annual Technical Meeting*, New York, May 1989, pp. 1150-1154.
31. T. S. Chow, *J. Chem. Phys.*, **79**(9), 4602 (1983).
32. J. G. Curro, R. R. Lagasse, and R. Simha, *Macromolecules*, **15**, 1621 (1982).
33. R. E. Robertson, *J. Polym. Sci., Polym. Phys. Ed.*, **17**, 597 (1979).

Received October 14, 1988

Accepted October 17, 1988